Journal of Chromatography, 538 (1991) 67–80
Elsevier Science Publishers B.V., Amsterdam

CHROM. 22 862

Cross-axis synchronous flow-through coil planet centrifuge (Type XLL)

II[a]. Speculation on the hydrodynamic mechanism in stationary phase retention

YOICHIRO ITO
Laboratory of Biophysical Chemistry, The National Heart, Lung, and Blood Institute, Building 10, Room 7N-322, National Institutes of Health, Bethesda, MD 20892 (U.S.A.)

ABSTRACT

The hydrodynamic mechanism involved in the retention of stationary phase in the present ×-axis coil planet centrifuge system is discussed. A statistical treatment of the retention data disclosed important clues such as the effect of the inward-outward elution mode, the close correlation between the planetary motion and the head–tail elution mode, and the superior retention capacity of the left-handed coils. The combined effects of the radial and lateral centrifugal force field derived from the mathematical analysis of acceleration acting on the coil provide an explanation for the phenomena.

INTRODUCTION

As described in Part I, a series of experiments has been performed to measure the retention of the stationary phase with various two-phase solvent systems using the present cross-axis (X-axis) coil planet centrifuge (CPC). The results obtained from these studies may be summarized as follows:

(1) The phase retention is affected by three major factors, *i.e.*, the direction of the planetary motion, the head–tail and inward–outward elution modes.

(2) With a few exceptions, two particular combinations of these factors yield high percentage retention for each choice of the mobile phase.

(3) The optimum combinations occur almost exclusively with left-handed coils.

In Part II, efforts are made to explain the above hydrodynamic phenomena. A simple statistical method was devised to isolate the hydrodynamic effects produced by each factor, and a set of force distribution diagrams derived for the planetary motion. These results were combined and used to discuss the hydrodynamic mechanism involved in the present X-axis CPC system.

[a] For Part I, see ref. 8.

0021-9673/91/$03.50

TABLE I

RETENTION (%) OF STATIONARY PHASE IN 7.6 cm HELICAL DIAMETER COIL

Mobile phase	Solvent System* 1 Hexane H_2O		2 Hexane MeOH		3 Hexane 1 EtOAc 1 MeOH 1 H_2O 1		4 EtO Ac H_2O		5 EtOAc 4 AcOH 1 H_2O 4	
	Condition**	%	Condition	%	Condition	%	Condition	%	Condition	%
Upper	P_{II}-T-I	91.4	P_I-T-I	66.5	P_I-T-I	80.7	P_I-T-I	86.8	P_I-T-I	82.7
	P_I-T-I	88.3	P_I-H-I	59.4	[illegible]	55.3	P_{II}-H-I	48.2	P_{II}-H-I	66.0
	P_{II}-T-O	58.4	P_I-H-I	38.1	P_I-T-O	55.3	P_I-H-I	42.1	P_{II}-T-I	45.2
	P_I-H-I	41.1	P_{II}-H-O	25.4	P_{II}-T-I	49.2	P_{II}-H-O	31.5	P_I-H-I	38.1
	P_{II}-H-I	35.5	P_{II}-T-I	21.8	P_I-H-I	42.1	P_{II}-T-I	15.7	P_{II}-H-O	25.4
	P_{II}-H-O	25.4	P_{II}-T-O	1.1	[illegible]	34.5	P_I-H-O	5.1	P_I-H-O	9.6
	P_I-H-O	18.3	P_I-H-O	1.0	P_{II}-H-O	31.5	P_{II}-T-O	2.5	P_I-T-O	0
	P_I-T-O	0	P_I-T-O	0	[illegible]	29.9	P_I-T-O	0	P_{II}-T-O	0
Lower	P_I-T-O	86.3	P_{II}-T-O	77.2	P_I-H-O	68.5	P_I-H-O	79.2	P_{II}-T-O	78.6
	P_{II}-H-O	69.5	P_I-H-O	66.0	P_{II}-H-O	58.9	P_{II}-T-O	78.2	P_I-H-O	74.1
	P_I-H-O	61.9	P_{II}-H-O	52.8	P_I-H-I	48.7	P_{II}-H-O	52.3	P_{II}-H-O	55.8
	P_I-H-I	50.8	P_I-H-I	44.2	[illegible]	39.1	P_I-H-I	32.5	P_I-H-I	28.9
	P_{II}-H-I	48.7	P_I-T-O	12.2	P_I-T-O	27.9	P_I-T-O	30.5	P_I-T-O	21.3
	P_I-T-O	12.7	P_{II}-T-I	10.7	P_{II}-T-I	15.2	P_I-T-I	26.4	P_{II}-T-I	9.1
	P_{II}-T-I	3.0	P_{II}-H-I	0	[illegible]	14.2	P_{II}-H-I	17.8	P_I-T-I	5.1
	P_I-T-I	0	[illegible]	0	[illegible]	0	P_{II}-T-I	2.5	[illegible]	1.0

Mobile phase	6 $CHCl_3$ H_2O		7 $CHCl_3$ 2 AcOH 2 H_2O 1		8 n-BuOH H_2O		9 n-BuOH 4 AcOH 1 H_2O 5		10 sec.-BuOH H_2O	
	Condition	%	Condition	%	Condition	%	Condition	%	Condition	%
Upper	P_I-T-I	66.0	P_I-T-I	87.3	P_I-T-I	71.1	[illegible]	65.5	[illegible]	73.6
	P_I-T-O	52.3	P_{II}-H-I	51.3	P_I-H-I	50.8	[illegible]	53.8	[illegible]	54.8
	P_{II}-H-I	50.8	P_I-H-I	46.7	P_I-H-I	44.7	P_{II}-T-I	50.3	P_{II}-T-I	48.2
	P_I-H-I	43.1	P_I-T-O	35.5	P_{II}-T-I	38.1	P_I-H-I	47.7	P_I-H-I	47.2
	P_I-H-O	39.1	P_{II}-H-O	28.4	P_{II}-H-O	27.9	P_{II}-H-O	29.9	P_{II}-H-O	27.9
	P_I-T-O	35.5	P_I-T-O	24.4	P_I-H-O	25.9	[illegible]	16.2	[illegible]	7.6
	P_{II}-T-I	25.9	P_I-H-O	17.8	P_I-T-O	17.8	P_I-T-O	2.5	[illegible]	0
	P_{II}-H-O	24.9	P_{II}-T-I	10.2	P_I-T-O	1.0	[illegible]	0	P_I-T-O	0
Lower	P_{II}-H-O	73.6	P_I-H-O	71.1	P_I-H-O	68.0	[illegible]	80.2	[illegible]	77.2
	P_I-H-O	66.0	P_{II}-H-O	59.9	P_I-H-O	63.5	[illegible]	68.5	[illegible]	64.5
	P_{II}-T-I	55.8	P_{II}-T-O	48.7	P_{II}-H-O	60.9	P_{II}-H-O	56.3	P_{II}-H-O	54.3
	P_I-H-I	53.3	P_I-H-I	40.6	P_I-T-O	45.2	P_I-T-O	53.3	P_I-T-O	44.7
	P_{II}-T-O	45.7	P_{II}-H-I	38.1	P_{II}-H-I	42.6	P_I-H-I	33.0	P_I-H-I	29.9
	P_I-T-O	35.5	P_I-T-O	37.6	P_I-H-I	41.6	[illegible]	18.3	[illegible]	16.8
	P_{II}-H-I	20.8	P_{II}-T-I	35.5	P_{II}-T-I	9.6	P_{II}-T-I	10.2	P_{II}-T-I	10.2
	P_{II}-T-I	1.5	P_{II}-T-I	2.5	P_I-T-I	2.5	[illegible]	0	[illegible]	1.0

* MeOH = methanol; EtOAc = ethyl acetate; AcOH = acetic acid; BuOH = butanol.

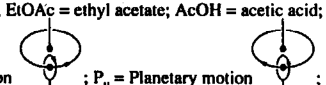

** P_I = Planetary motion [diagram] ; P_{II} = Planetary motion [diagram] ;
H = Head to tail elution; T = Tail to head elution; I = Inward elution; O = Outward elution
Plain background = Right-handed coil; Shaded background = Left-handed coil.

ANALYSIS OF PHASE RETENTION DATA

A set phase retention data obtained from the coil mounted on the two different holders at 800 rpm are listed in Table I (7.6 cm diameter holder) and II (24 cm diameter holder). Each table shows percentage retention of the stationary phase for ten pairs of two-phase solvent systems with both upper and lower phases used as the mobile phase. Each column contains eight retention data obtained from the indicated solvent system under the experimental conditions expressed by combinations of three factors, *i.e.*, the direction of planetary motion (P_I and P_{II}) (see Table I bottom for definitions), the head–tail elution mode (H: head to tail and T: tail to head), and the direction of elution along the column axis (I: inward and O: outward). These data are arranged from top to bottom in decreasing order of phase retention. The results obtained from the left-handed coils are shaded.

The overall results indicate that all eight experimental conditions yield somewhat different levels of retention in each solvent system and that the data from the left-handed coils (shaded) dominate in both tables. However, the interrelation of these factors is quite complex and difficult to rationalize without additional statistical treatment.

In order to elucidate the hydrodynamic mechanism involved in the present system, it is highly desirable to isolate the effects produced by each individual factor on the retention of the stationary phase. This can be done by considering the three sets of diagrams shown in Figs. 1–3. Each diagram shows the retention with one combination of the three factors plotted on the horizontal axis against another combination with only one factor different on the vertical axis. This is done for each of the three factors, namely, the planetary motions P_I vs P_{II} (Fig. 1); the head-to-tail elution *vs.* tail-to-head elution (Fig. 2); and the inward elution *vs.* outward elution (Fig. 3). Each set of these figures includes a total of four graphs showing the phase retention in both 7.6 cm (A) and 24 cm (B) helical diameter coils each with the upper (left) and the lower (right) phases used as the mobile phase.

Fig. 1A shows a pair of diagrams obtained by plotting the percentage phase retention of P_I *vs.* P_{II} for the lower (left) and the upper (right) phases. For convenience each diagram is divided by three lines; thin horizontal and vertical lines divide the whole area into four equal squares where the upper right square indicates satisfactory retention from both planetary motions; the right lower and upper squares indicate satisfatory retention from P_I and P_{II}, respectively; and the left lower square, unsatisfactory retention regardless of the applied mode of planetary motion. Each diagram is also divided into two equal triangles by a thick diagonal line, which provides the most important information in the present analysis: The data points located on or near the diagonal line indicate that the planetary motion produces no significant effect on the retention. The deviation of the point above the line indicates a positive effect from P_{II}, or negative effect from P_I, or the combination on the phase retention, and *vice versa* if the point is below the diagonal line. The distance of the points from the diagonal line indicates the relative magnitude of the effect.

Each diagram contains 40 data points with specific symbols assigned to four combinations between the remaining two factors, *i.e.*, open circles for the head-to-tail elution and solid circles for the tail-to-head elution each with arrows directing toward the left to indicate outward elution and toward the right to indicate inward elution. All

TABLE II

RETENTION (%) OF STATIONARY PHASE IN 24 cm HELICAL DIAMETER COIL

Mobile phase	*Solvent System**																			
	1 *Hexane* H_2O		*2* *Hexane* *MeOH*		*3* *Hexane 1* *EtOAc 1* *MeOH 1* H_2O *1*		*4* *EtOAc* H_2O		*5* *EtOAc 4* *AcOH 1* H_2O *4*		*6* $CHCl_3$ H_2O		*7* $CHCl_3$ *2* *AcOH 2* H_2O *1*		*8* *n-BuOH* H_2O		*9* *n-BuOH 4* *AcOH 1* H_2O *5*		*10* *sec.-BuOH* H_2O	
	*Condition***	*%*	*Condition*	*%*	*Condition*	*%*	*Condition*	*%*	*Condition*	*%*	*Condition*	*%*	*Condition*	*%*	*Condition*	*%*	*Condition*	*%*	*Condition*	*%*
Upper	P_{I}-T-I	96.5	P_{II}-H-I	84.8	P_{I}-T-I	93.3	P_{II}-H-I	83.0	P_{II}-H-I	70.0	P_{I}-T-I	95.8	P_{I}-T-I	87.3	P_{I}-T-I	84.8	P_{II}-H-I	49.8	P_{II}-H-O	55.5
	P_{I}-T-O	94.3	P_{I}-T-I	82.7	P_{I}-T-O	90.5	P_{I}-T-I	74.6	P_{I}-T-I	68.9	P_{I}-T-O	93.3	P_{I}-T-O	58.0	P_{I}-T-O	83.0	P_{II}-H-O	44.5	P_{II}-H-I	48.1
	P_{II}-H-I	52.3	P_{II}-H-O	77.4	P_{II}-H-I	49.8	P_{II}-H-O	71.4	P_{II}-H-O	60.8	P_{II}-H-I	46.3	P_{II}-H-I	48.1	P_{II}-H-O	51.2	P_{I}-H-I	35.7	P_{I}-H-I	43.8
	P_{II}-H-O	42.4	P_{I}-T-O	46.6	P_{II}-H-O	41.0	P_{I}-T-O	44.5	P_{I}-T-O	39.6	P_{II}-H-O	38.9	P_{II}-H-O	43.5	P_{II}-H-I	48.8	P_{I}-H-O	30.4	P_{I}-T-O	31.1
	P_{II}-T-I	30.4	P_{I}-H-I	24.4	P_{II}-T-I	18.7	P_{I}-H-I	28.6	P_{I}-H-I	31.4	P_{II}-T-I	20.5	P_{I}-H-I	12.7	P_{II}-T-I	21.2	P_{I}-T-I	22.6	P_{I}-H-O	26.9
	P_{I}-H-I	1.0	P_{I}-H-O	6.4	P_{I}-H-I	12.7	P_{I}-H-O	10.2	P_{I}-H-O	15.2	P_{I}-H-I	4.6	P_{II}-T-I	12.7	P_{I}-H-I	20.5	P_{I}-T-O	19.8	P_{II}-T-I	19.8
	P_{I}-H-O	0	P_{II}-T-I	0	P_{I}-H-O	6.4	P_{II}-T-I	0	P_{II}-T-I	11.7	P_{I}-H-O	1.1	P_{I}-H-O	8.8	P_{I}-H-O	14.1	P_{II}-T-I	16.3	P_{I}-T-I	9.9
	P_{II}-T-O	0	P_{II}-T-O	0	P_{II}-T-O	0	P_{II}-T-O	0	P_{II}-T-O	0	P_{II}-T-O	0	P_{II}-T-O	0	P_{II}-T-O	1.4	P_{II}-T-O	0	P_{II}-T-O	0
Lower	P_{I}-H-O	93.6	P_{II}-T-O	83.7	P_{I}-H-O	86.9	P_{II}-T-O	94.0	P_{II}-T-O	75.3	P_{I}-H-O	94.7	P_{II}-T-O	87.6	P_{I}-H-O	73.5	P_{I}-T-O	64.0	P_{II}-H-O	52.3
	P_{II}-T-O	90.5	P_{II}-T-I	74.6	P_{I}-H-I	65.7	P_{II}-T-I	72.8	P_{I}-H-O	61.5	P_{II}-T-O	94.0	P_{I}-H-O	86.6	P_{I}-H-I	72.8	P_{II}-T-O	53.4	P_{II}-T-O	50.9
	P_{I}-H-I	90.5	P_{I}-H-O	68.9	P_{II}-T-O	53.4	P_{I}-H-O	69.3	P_{II}-T-I	46.6	P_{I}-H-I	91.2	P_{I}-H-I	62.2	P_{II}-T-O	58.7	P_{I}-H-O	47.0	P_{I}-T-O	48.1
	P_{II}-T-I	45.9	P_{I}-H-I	46.3	P_{II}-H-O	36.4	P_{I}-H-I	38.9	P_{I}-H-I	28.6	P_{II}-H-O	44.5	P_{II}-T-I	38.2	P_{II}-H-O	44.9	P_{II}-H-O	32.2	P_{I}-H-O	37.1
	P_{II}-H-O	38.9	P_{I}-T-O	15.5	P_{II}-H-I	32.1	P_{I}-T-O	24.0	P_{I}-T-O	25.8	P_{II}-H-I	29.0	P_{II}-H-O	31.1	P_{II}-H-I	32.2	P_{II}-T-I	30.4	P_{II}-H-I	29.0
	P_{II}-H-I	20.1	P_{I}-T-I	6.4	P_{II}-T-I	18.0	P_{I}-T-I	10.2	P_{I}-T-I	13.4	P_{II}-T-I	25.8	P_{II}-H-I	28.6	P_{II}-T-I	28.6	P_{II}-H-I	28.6	P_{II}-T-I	19.8
	P_{I}-T-O	0	P_{II}-H-O	4.2	P_{I}-T-O	9.2	P_{II}-H-O	5.6	P_{II}-H-O	12.7	P_{I}-T-O	6.7	P_{I}-T-O	9.9	P_{I}-T-O	16.3	P_{I}-T-I	17.0	P_{I}-T-I	18.4
	P_{I}-T-I	0	P_{II}-H-I	1.1	P_{I}-T-I	3.0	P_{II}-H-I	0	P_{II}-H-I	0	P_{I}-T-I	3.2	P_{I}-T-I	3.5	P_{I}-T-I	8.5	P_{I}-H-I	14.1	P_{I}-H-I	15.9

* & ** See caption in TABLE I.

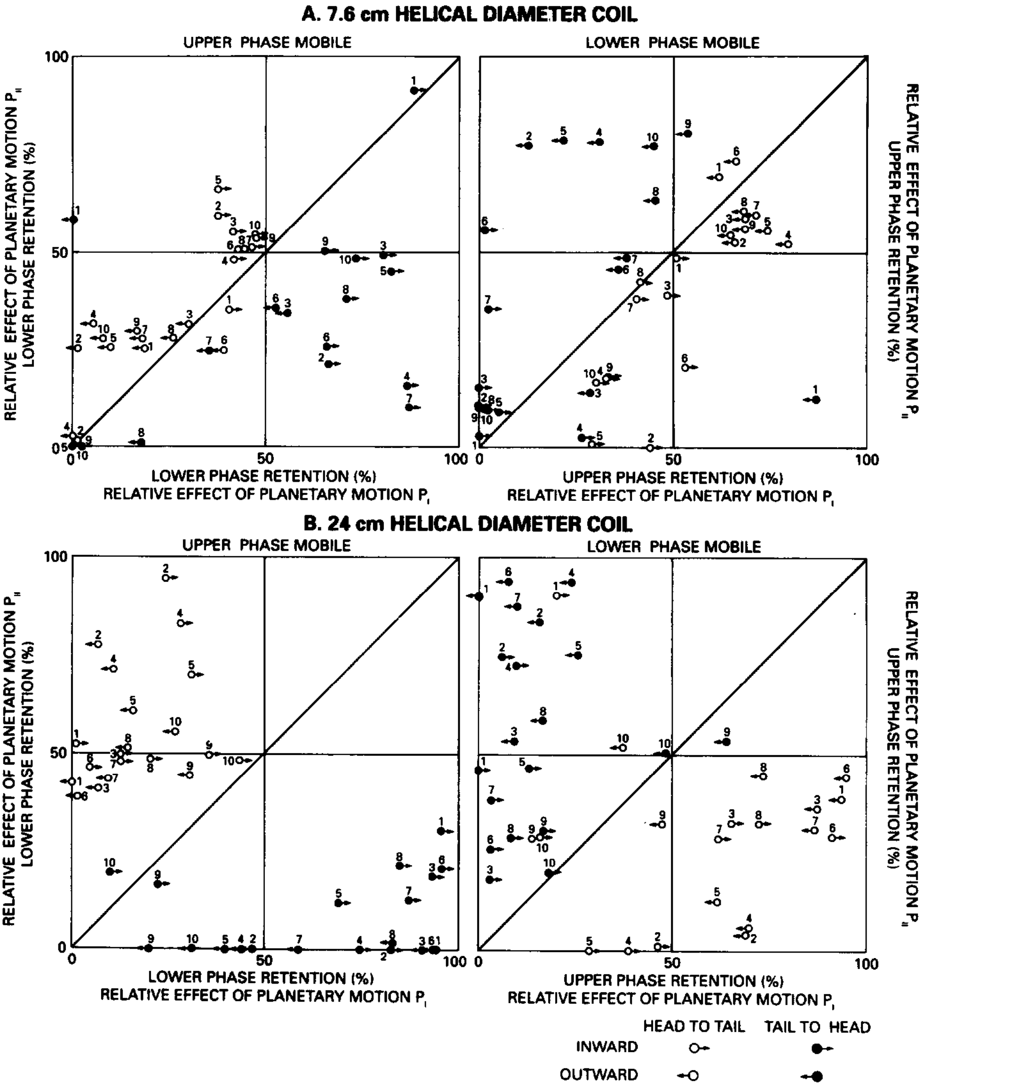

Fig. 1. Effects of planetary motion P_I and P_{II} on the retention of the stationary phase. (A) 7.6 cm helical diameter coil; (B) 24 cm helical diameter coil; left: upper phase mobile; right: lower phase mobile.

these points are also numbered from 1 to 10 to indicate the applied two-phase solvent systems (see Table I for identification of the solvent systems).

Observation on Fig. 1 clearly reveals that the data points are divided into two groups by the diagonal line. With a few exceptions, the open circles are distributed above the diagonal line and the solid circles below the line if the upper phase is mobile (left), this relationship is reversed if the lower phase is mobile (right). This indicates that the retention of the lower phase is enhanced by the combination of either planetary motion P_{II} and the head-to-tail elution (P_{II}-H) or planetary motion P_I and the

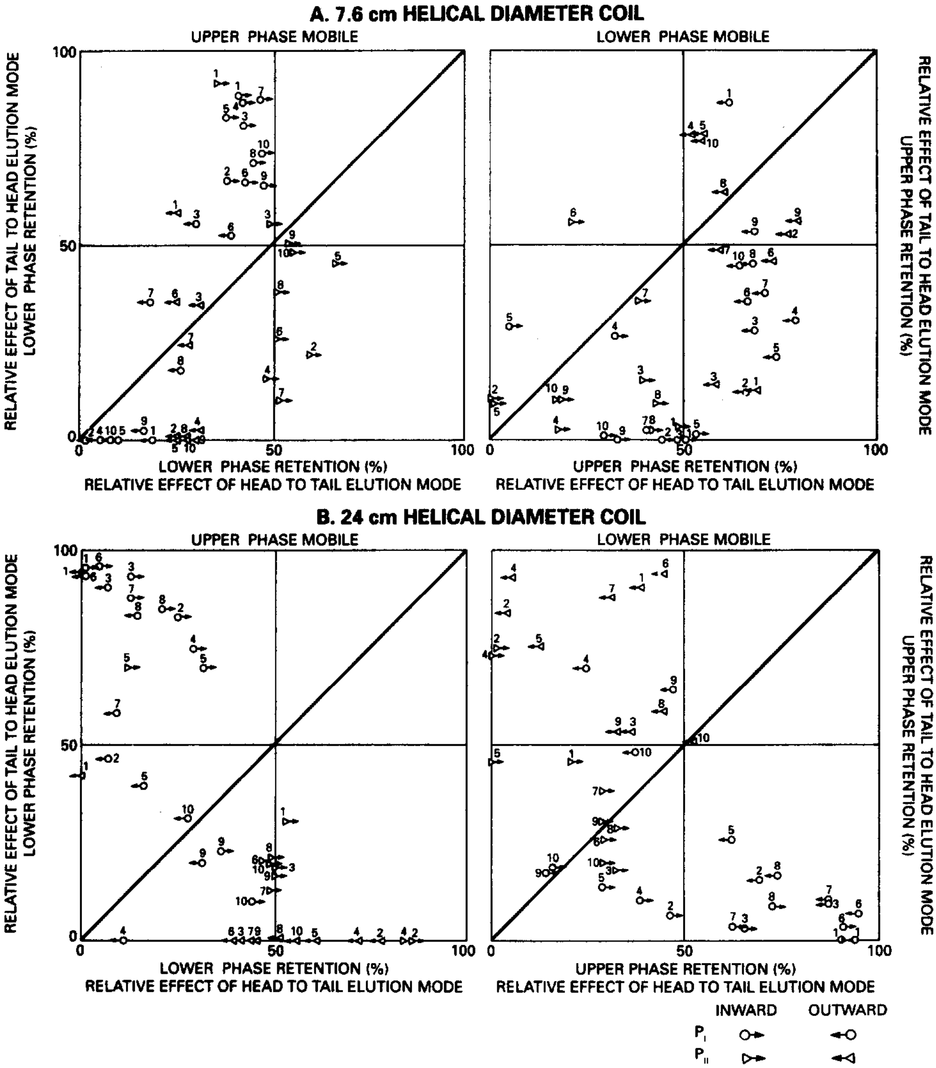

Fig. 2. Effects of the head–tail elution mode on the retention of the stationary phase. (A) 7.6 cm helical diameter coil; (B) 24 cm helical diameter coil; left: upper phase mobile; right: lower phase mobile.

tail-to-head elution (P_I-T) whereas the retention of the upper phase is similarly enhanced by the combination of either planetary motion P_I and the head-to-tail elution (P_I-H) or planetary motion P_{II} and the tail-to-head elution (P_{II}-T). In either case, the retention tends to increase in the larger diameter coil as evidenced by the greater deviation of each point from the diagonal line in the 24 cm helical diameter coil. These results indicate a close correlation between the planetary motion and the head-tail elution mode in the stationary phase retention while no significant correlation is observed between the planetary motion and the inward-outward elution mode.

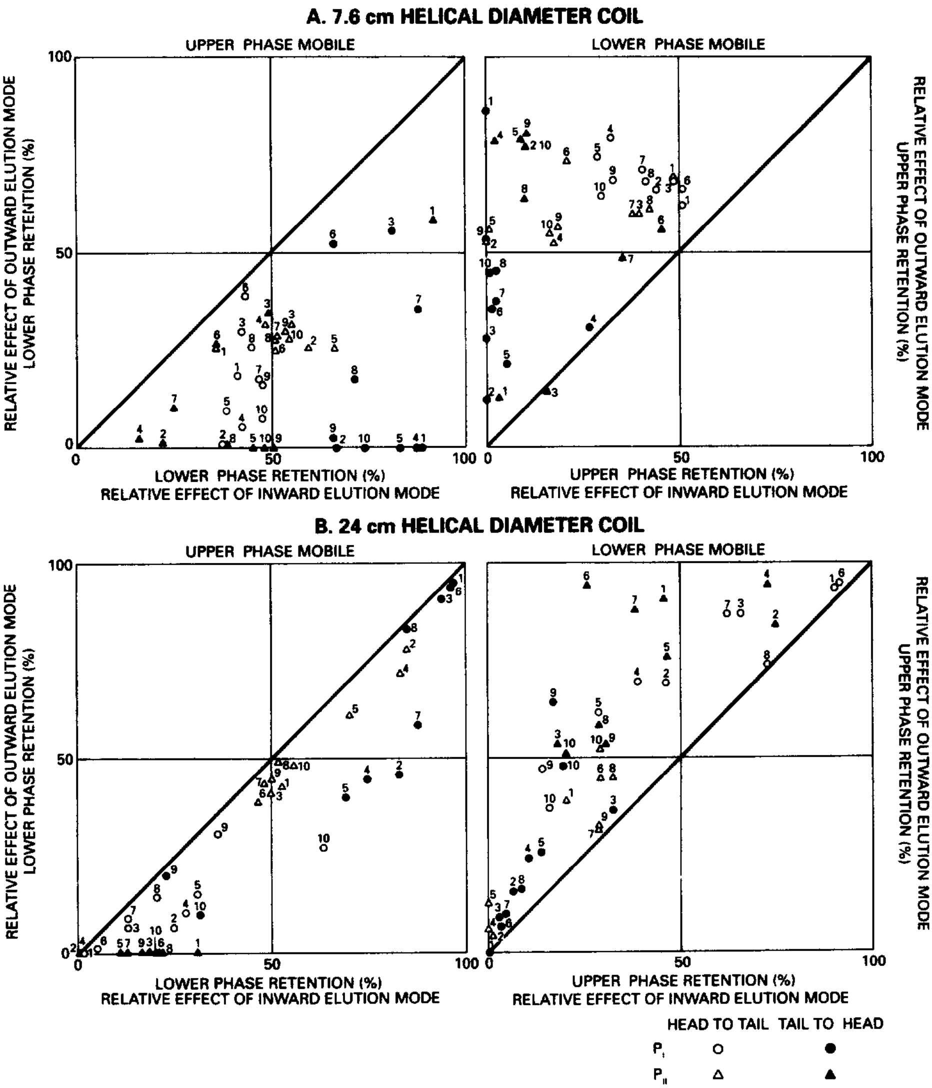

Fig. 3. Effects of the inward–outward elution mode on the retention of the stationary phase. (A) 7.6 cm helical diameter coil; (B) 24 cm helical diameter coil; left: upper phase mobile; right: lower phase mobile.

However, there are some exceptions; the correlation between the planetary motion and the head-tail elution mode is relatively weak among the viscous low interfacial tension butanol solvent systems (9 and 10) as indicated by location of these points near the diagonal line in the 24 cm helical diameter coil. Also, the high interfacial tension hexane–water system (1) shows an aberrant retention pattern in 7.6 cm helical diameter coil.

Figs. 2A and B similarly illustrate the effects of the head-tail elution mode on the stationary phase retention where the 40 data points are plotted with symbols assigned to four different combinations of the planetary motion and the inward-outward elution mode as indicated at the bottom of the diagrams. These points are also numbered to facilitate identification of the applied two-phase solvent systems (see Table I).

In both 7.6 and 24 cm helical diameter coils combinations P_I-I (open circles with arrows directing toward the right) are mostly located in the left upper squares for the lower phase retention (left) while combinations P_{II}-O (open circles with arrows directing toward the left) dominate the right lower square for the upper phase retention (right). Here again the close correlation between the planetary motion and the head–tail elution mode is confirmed. The deviation of the points from the diagonal is also enhanced in the large helical diameter coils. In the 24 cm helical diameter coil (Fig. 2B right), combinations P_{II}-O (open triangles with arrows directing toward the left) also dominate in the left upper square indicating that the retention of the upper phase is remarkably improved by the combination of P_{II} and the outward elution in the large helical diameter coil.

Finally, Figs. 3A and B illustrate the effects of the inward–outward elution mode on the stationary phase retention where the 40 data points are similarly plotted with symbols corresponding to the four different combinations as specified at the bottom of the diagrams. As in other diagrams, all points are numbered to facilitate identification of the two-phase solvent systems used.

In contrast with other diagrams (Figs. 1 and 2), all the present diagrams show unilateral distribution of the data points with respect to the diagonal line. Except for a single data point, all points are located below the diagonal line if the upper phase is mobile (left) and above the diagonal line if the lower phase is mobile (right), indicating that eluting either the upper phase inward or the lower phase outward enhances the stationary phase retention under any combination with other factors in both 7.6 and 24 cm helical diameter coils. The deviation of each data point from the diagonal line is much greater in the 7.6 cm helical diameter coil, suggesting that this tendency is enhanced in the small helical diameter coils.

The overall results of the above analyses indicate that all three factors play important roles in the retention of the stationary phase in the present X-axis CPC. The hydrodynamic effects of the planetary motion and the head-tail elution mode are closely interrelated in such a way that the high retention levels are obtained by choosing the particular combinations of these two factors, *i.e.*, P_I-T or P_{II}-H for the upper phase mobile and the P_{II}-T or P_I-H for the lower phase mobile. On the other hand, the third factor of the inward–outward elution mode is rather independent of the above two factors and exclusively related to the choice of the mobile phase: the high percentage retention was achieved by eluting either the upper phase inward or the lower phase outward through the coil.

Consequently, the highest retention levels are generally provided from two combinations (among the eight possible combinations) for each choice of the mobile phase: P_I-T-I and P_{II}-H-I for the upper mobile phase and P_{II}-T-O and P_I-H-O for the lower mobile phase. As shown in Table I, these four combinations are exclusively provided by the use of left-handed coils.

FORCE DISTRIBUTION DIAGRAMS

Fig. 4 shows the orientation and motion of the coil holder in the present X-axis

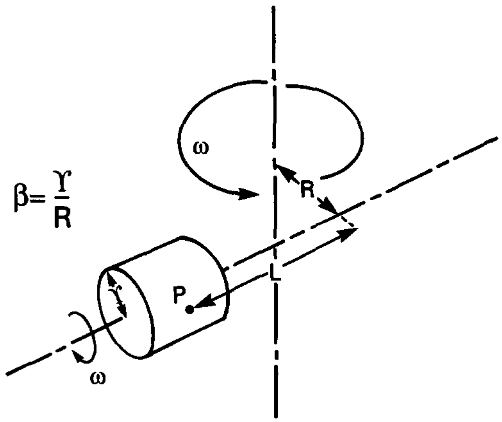

Fig. 4. Planetary motion of the coil holder in the present X-axis CPC.

CPC system. Analysis of acceleration acting on an arbitrary point, P, on the holder was previously performed by the aid of a three-dimensional coordinate system [1,2]. The acceleration acting on the holder was finally transferred to the x_b–y_b–z_b body coordinate system and expressed in the following equations:

$$\alpha_{xb} = -R\omega^2 (1 - 2\beta \cos \theta) \quad (1)$$

$$\alpha_{yb} = -R\omega^2 \beta \sin \theta \quad (2)$$

$$\alpha_{zb} = -R\omega^2 2\beta \sin \theta + L\omega^2 \quad (3)$$

where α_{xb}, α_{yb}, and α_{zb} are acceleration components acting along the indicated coordinates; R is the radius of revolution; ω is the angular velocity ($\theta = \omega t$); $\beta = r/R$ where r is the distance from the holder axis to the coil; and L is the lateral disposition of the coil expressed by the distance from the center of the holder shaft to the coil holder.

Using these equations, the centrifugal force vectors (same magnitude as the acceleration but acting in the opposite direction) at various locations on the holder were computed for three types to planetary motions, *i.e.*, type X ($L = 0$), type XL ($-L = R$), and type XLL ($-L = 2R$) and diagrammatically illustrated in Fig. 5A–C. In these force distribution diagrams, the three-dimensional distribution of the centrifugal force vectors are expressed on a two-dimensional diagram by combining the two force vectors, $-\alpha_{xb}$ and $-\alpha_{yb}$, into a single arrow forming various angles from the x_b-axis, whereas the third force vector, $-\alpha_{zb}$, which acts perpendicularly to the x_b–y_b plane, is drawn as a vertical column along the y_b-axis. The ascending column indicates the force acting upward ($z_b > 0$) and the descending column, the force acting downward ($z_b < 0$). Several concentric circles around point O_b (the axis of the holder) indicate locations on the holder corresponding to parameter β indicated in the diagram. The distribution of the centrifugal force vectors in each diagram is fixed to the x_b–y_b–z_b body coordinate system and every point on the holder rotates around point O_b (z_b-axis) in either clockwise or counterclockwise direction as determined by the planetary motion of the holder.

In these diagrams, the radially directed centrifugal force vectors (expressed by arrows) display an asymmetrical distribution pattern along the x_b-axis which is

A. FORCE DISTRIBUTION AT L = 0 (TYPE X)

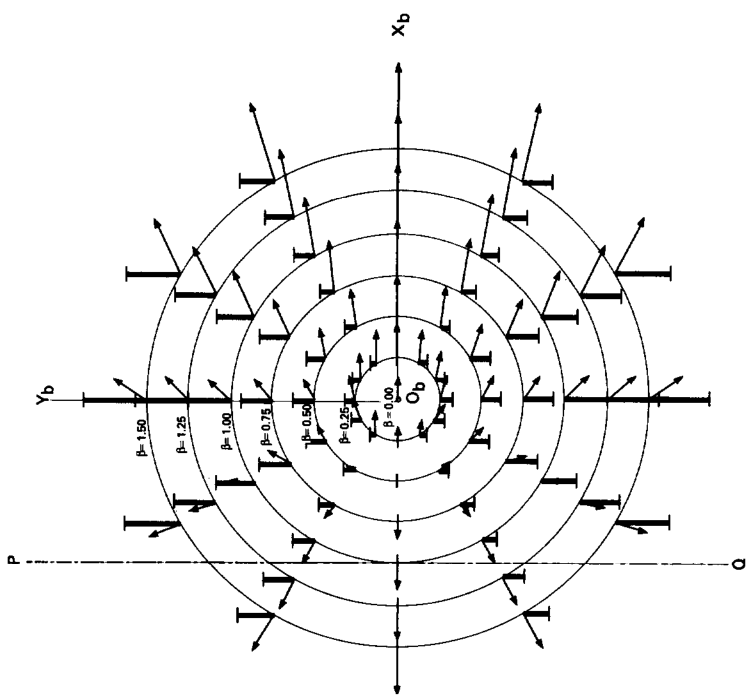

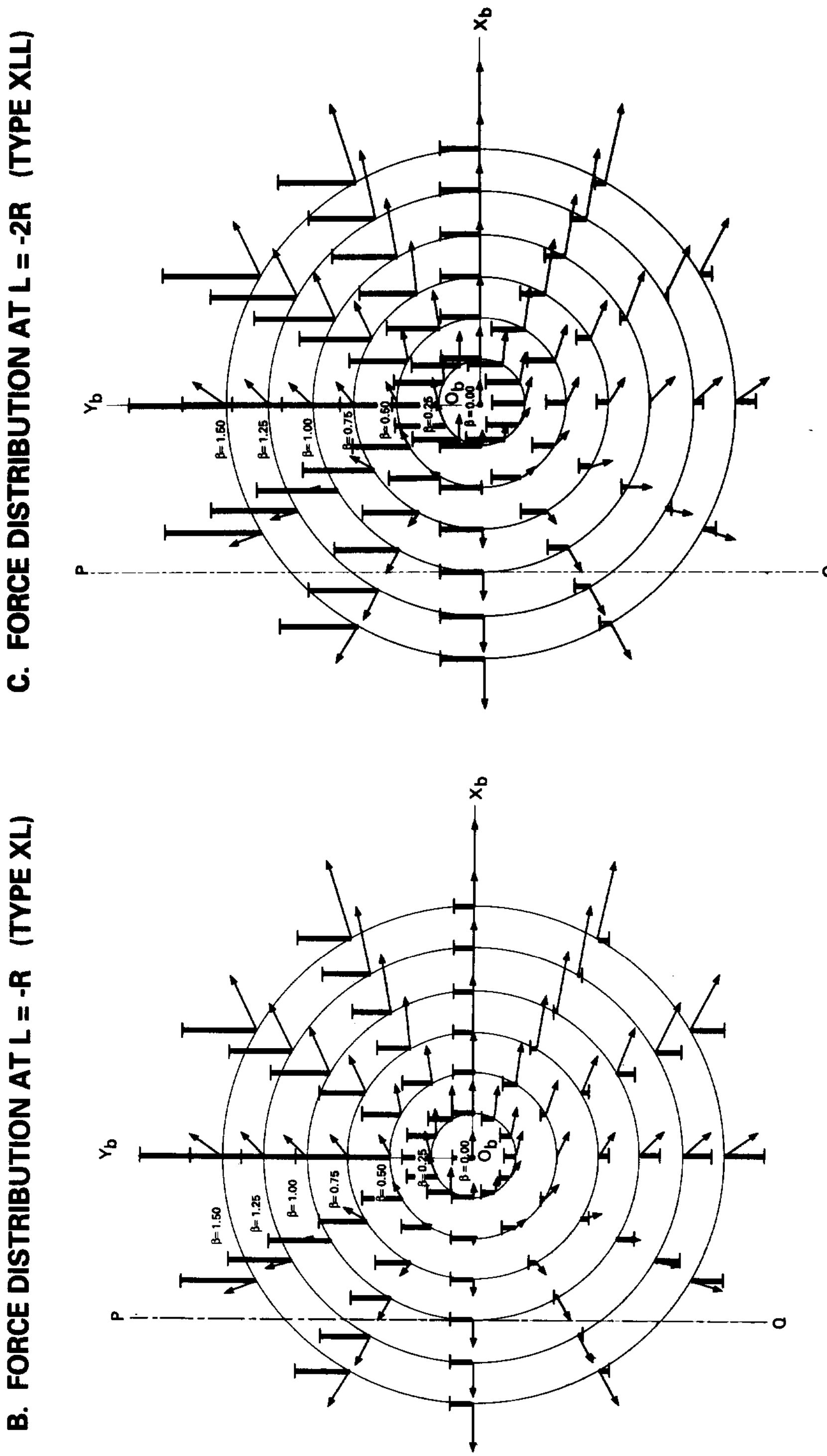

Fig. 5. Force distribution diagrams of the X-axis CPC. (A) Type X; (B) type XL; (C) type XLL. $\overline{PQ}$: Axis of revolution (centrifuge axis).

unaltered by the change of the L values. The vertically acting centrifugal force vectors (expressed by columns), on the other hand, show a symmetrical distribution pattern at $L = 0$ (Fig. 5A), but the pattern changes according to the L values. At $-L=R$ (Fig. 5B), the force vectors acting upward on the upper half of the holder gain their magnitude whereas those acting downward at the lower half of the holder lose their strength, resulting in an asymmetrical distribution of the force vector along the z_b-axis. The degree of the asymmetry becomes greater at $-L=2R$(Fig. 5C) representing the present XLL system.

These force distribution diagrams may serve as a useful guide for discussion of the hydrodynamic effects occurring in the present X-axis CPC system.

SPECULATION OF HYDRODYNAMIC MECHANISM

The analysis of acceleration described above indicated that the centrifugal force field acting on the rotating holder is divided into two groups; the radial force field expressed by arrows and the lateral (tangential) force field expresed by vertical columns. For convenience, the following discussion may be divided into two parts, *i.e.*, the effects of the individual force fields and the combined effects of the two on the retention of the stationary phase.

The effects of the radial force field on the retention of the stationary phase have been extensively studied with the type J synchronous coil planet centrifuge which produces a similar asymmetric radial centrifugal force field without lateral components [3–7]. A series of studies has shown that two immiscible solvent phases are unilaterally distributed in the coil according to the physical properties of the solvent system. Hydrophobic binary solvent systems such as *n*-hexane–water and chloroform–water always distribute the upper phase toward the head side of the coil whereas the hydrophilic low-interfacial-tension solvent systems such as *n*-butanol–acetic acid–water (4:1:5) and *sec.*-butanol–water show the opposite hydrodynamic trend, distributing the lower phase toward the head side of the coil. In other solvent systems with intermediate physical properties, the head phase is determined by the β values of the coil; at large β values the upper phase is distributed to the head side while in small β values the lower phase is distributed on the head side. In the X-axis CPC, the strength of the radial force field is reduced by separation of the Coriolis force which is directed laterally along the axis of the holder.

On the other hand, the individual hydrodynamic effects produced by the lateral force field have not been well investigated. However, it is apparent that with the lateral coil position such as in the present X-axis CPC system the centrifugal force gradient formed along the holder axis may facilitate the retention of the stationary phase if the heavier phase is eluted outward (toward the left) or the lighter phase inward (toward the right) as observed in the present studies (see Fig. 3A and B). Consequently, in the conventional multilayer coil configuration, every other layer can hold a greater volume of the stationary phase in a given elution mode. However, in order to understand the superior retention capacity of the left-handed coil to the right-handed coil (see Tables I and II), one must consider the complex hydrodynamic interaction between the radial and lateral centrifugal force fields.

Fig. 6 schematically illustrates the hydrodynamic interaction between the radial and lateral force fields acting on the coils undergoing planetary motions P_I (left) and

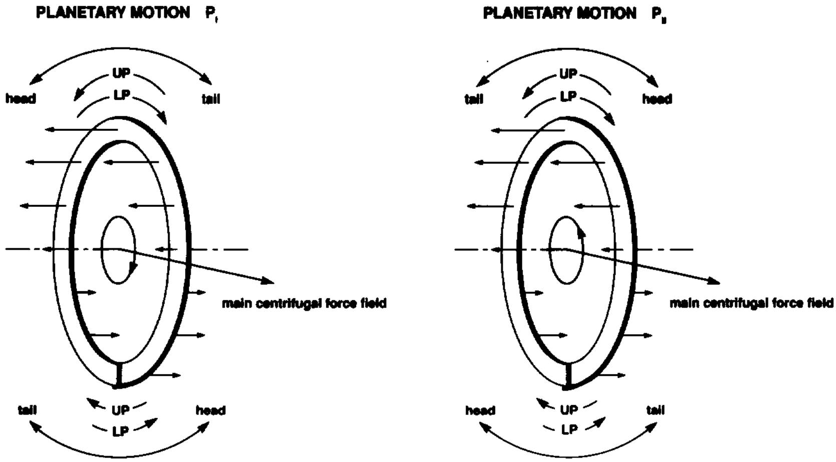

Fig. 6. Hydrodynamic effect of the radial and lateral centrifugal force fields in the present X-axis CPC. UP = Upper phase; LP = lower phase.

P_{II} (right) [2]. Because the directions of rotation and revolution are simultaneously reversed, these two planetary motions produce the identical centrifugal force field whereas reversed rotation of the coil holder causes reversal of the head-tail orientation of the coil. Under the main centrifugal force field directing radially toward the right as indicated by a large arrow, the upper (lighter) phase is driven toward the left and the lower (heavier) phase toward the right in major portions of the coil.

In Fig. 6 (left), planetary motion P_I determines the coil rotation, hence the head-tail orientation of the coil as indicated by a pair of curved arrows at the top and the bottom of the diagram. Owing to the asymmetric lateral force field between the

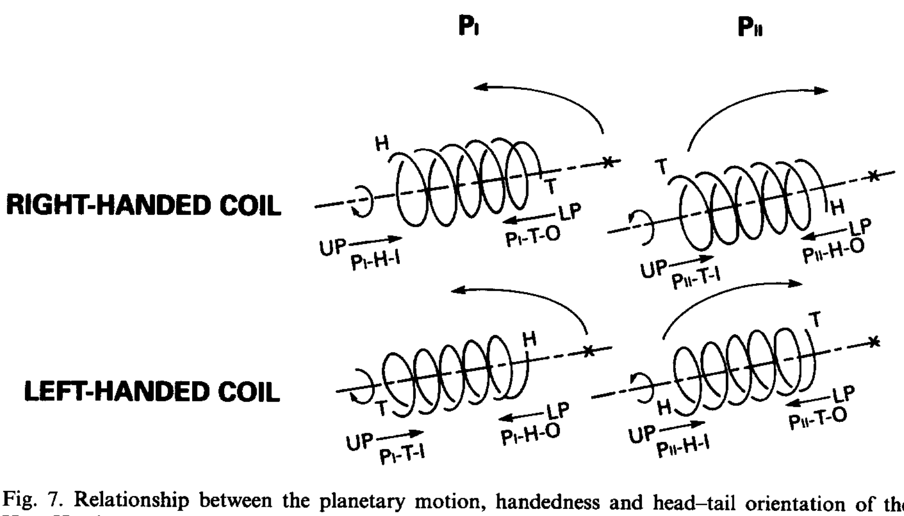

Fig. 7. Relationship between the planetary motion, handedness and head–tail orientation of the coil. H = Head; T = tail; UP = upper phase; LP = lower phase. I = inward elution; O = outward elution; × = the center of the rotary shaft.

upper and lower halves of the coil, the counter-current movement of the two solvent phases is accelerated in the upper portion of the coil owing to suppressed emulsification while the movement is decelerated in the lower portion of the coil owing to enhanced emulsification. Consequently, in this situation the tail-to-head elution (P_I-T) of the upper phase and the head-to-tail elution (P_I-H) of the lower phase results in enhanced retention of the stationary phase.

In Fig. 6 (right), planetary motion P_{II} reverses both the rotation and the head-tail orientation of the coil as illustrated. Owing to the asymmetric lateral force field left unaltered, the counter-current movement of the two solvent phases is similarly accelerated on the upper portion of the coil and decelerated in the lower portion of the coil. Therefore, in this case the head-to-tail elution (P_{II}-H) of the upper phase and the tail-to-head elution (P_{II}-T) of the lower phase result in enhanced retention of the stationary phase.

The above hydrodynamic mechanism provides reasonable explanation for the close correlation between the planetary motion and the head-tail elution mode observed in the present studies (Figs. 1 and 2). The radial force field may also play an additional role in stationary phase retention. For example, in the 7.6 cm helical diameter coil, the best retention of the lower phase is obtained by P_I-T-I, probably due to the effect of the radial force field which distributes the upper phase toward the head of the coil. An atypical retention pattern of hexane–water in the 7.6 cm helical diameter coil may indicate a possible inhibitory effect of the lateral force field on the counter-current flow of particular two-phase solvent systems with extremely high interfacial tension.

Fig. 7 shows the relationship between the planetary motion, handedness and head–tail orientation of the coils undergoing the XLL planetary motion as indicated by curved arrows. As illustrated by four different diagrams, the head-tail orientation of the coil is determined by the combination of handedness and planetary motion. Since the stationary phase retention is enhanced by eluting either the upper phase inward or the lower phase outward through the coil as indicated by straight arrows, the desirable combinations of P_I-T-I and P_{II}-H-I for the lower phase retention and those of P_I-H-O and P_{II}-T-O for the upper phase retention are all available only from the left-handed coils.

ACKNOWLEDGEMENT

The author of this paper wishes to thank Dr. Henry M. Fales for his assistance in reviewing this paper.

REFERENCES

1 Y. Ito, *Sep. Sci. Technol.*, 22 (1987) 1971.
2 Y. Ito and T.-Y. Zhang, *J. Chromatogr.*, 449 (1988) 135.
3 Y. Ito, *J. Chromatogr.*, 301 (1984) 377.
4 Y. Ito, *J. Chromatogr.*, 301 (1984) 387.
5 Y. Ito and W. D. Conway, *J. Chromatogr.*, 301 (1984) 405.
6 Y. Ito, *CRC Crit. Rev. Anal. Chem.*, 17 (1986) 65.
7 Y. Ito, in N. B. Mandava and Y. Ito (Editors), *Countercurrent Chromatography—Theory and Practice*, Marcel Dekker, New York, 1988, Ch. 3, pp. 79–442.
8 Y. Ito, E. Kitazume, M. Bhatnagar and F. D. Trimble, *J. Chromatogr.*, 538 (1991) 59.